Harnessing Janus Nanoparticles to Create Controllable Pores in Membranes

Alexander Alexeev,[†] William E. Uspal,[‡] and Anna C. Balazs[§,*]

[†]George W. Woodruff School of Mechanical Engineering, Georgia Institute of Technology, Atlanta, Georgia 30332, [‡]Department of Physics, MIT, Cambridge, Massachusetts 02139, and [§]Chemical Engineering Department, University of Pittsburgh, Pittsburgh, Pennsylvania 15261

ABSTRACT We use a coarse-grained numerical simulation to design a synthetic membrane with stable pores that can be controllably opened and closed. Specifically, we use dissipative particle dynamics to probe the interactions between lipid bilayer membranes and nanoparticles. The particles are nanoscopic Janus beads that comprise both hydrophobic and hydrophilic portions. We demonstrate that when the membrane rips and forms a hole due to an external stress, these nanoparticles diffuse to the edge of the hole and form a stable pore, which persists after the stress is released. Once the particle-lined pore is formed, a small increase in membrane tension readily reopens the pore, allowing transport through the membrane. Besides the application of an external force, the membrane tension can be altered by varying, for example, temperature or pH. Thus, the findings provide guidelines for designing nanoparticle-bilayer assemblies for targeted delivery, where the pores open and the cargo is released only when the local environmental conditions reach a critical value.

KEYWORDS: lipid membrane · Janus nanoparticles · controllable pore · computer simulations

Lipid bilayer membranes play a vital role in maintaining the structural integrity of biological cells and synthetic vesicles, as well as regulating the passage of small molecules in and out of these entities. Typically, the membrane will stretch in response to external forces, but above a critical force, it splits open and forms a pore, which enables the transport of solvent through the system. Yet once the external force is removed, the fluidity of the bilayer causes the pore to close and effectively disappear. For various technological applications, however, it would be useful to design a "smart membrane" that not only forms a stable pore, but also can open and close this pore "on demand". Such membranes could pave the way for creating novel self-healing materials, breathable fabrics, and assemblies for controlled drug delivery.

Herein, we use computer simulations to add Janus nanoparticles, which contain both hydrophobic and hydrophilic portions, to the solution surrounding a lipid bilayer membrane. As we show below, the addition of these particles leads to the formation of stable, "reusable" pores within the bilayer. In particular, when the membrane splits open under an applied tension, the Janus particles self-assemble at the internal edges of this pore and thereby, stabilize the opening. When the tension is removed, the nanoparticles remain in their energetically favored position within the pore. Consequently, when the tension is reapplied, the stable pore reappears. Furthermore, the amount of force needed to open the particle-lined pore is less than that required to initially produce a hole within the membrane. In effect, the self-assembled Janus particles act as a "zipper", which allows a specific slit to be repeatably opened or closed.

The Janus nanoparticle self-assembly described above also mimics the behavior of certain peptides and proteins, which form and stabilize channels in biological bilayers.[1] In this study, we attempt to establish optimal conditions for harnessing the Janus nanoparticles to act as "artificial proteins", which would allow us to create gateways and regulate the trafficking of molecules into and out of synthetic membranes and vesicles.

We note that the existing theoretical[2–10] and computational[11–13] studies on nanoparticle-bilayer interactions have primarily examined how membranes can be driven to wrap around a particle. To the best of our knowledge, there have been no prior theories or simulations to probe the interactions of Janus particles and lipid bilayers.

To carry out this study, we use dissipative particle dynamics (DPD) simulations. The DPD is essentially a course-grained

See the accompanying Perspective by Yoshida and Lahann on p 1101.

*Address correspondence to balazs1@engr.pitt.edu.

Received for review February 17, 2008 and accepted April 30, 2008.

Published online May 15, 2008.
10.1021/nn8000998 CCC: $40.75

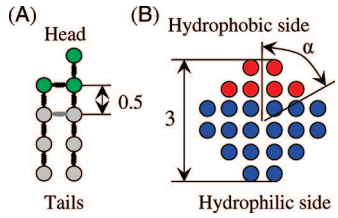

Figure 1. Architecture of the lipids (A) and Janus nanoparticles (B). In panel A, the green beads make up the hydrophilic headgroup in the lipid and the gray beads form the hydrophobic tails. The equilibrium separation between the beads is 0.5 (in DPD units). In panel B, the blue beads constitute the hydrophilic sites in the Janus nanoparticle, while the red beads are the hydrophobes. The height of the particle is 3 (in DPD units).

molecular dynamics (MD) method that allows researchers to examine larger systems in more computationally realistic time frames.[14] The technique has proven to be especially useful in studying the mesoscale behavior of bilayer membranes.[14–22] The DPD method has been detailed extensively elsewhere,[23] so herein we provide only a brief description of the technique in the Methods section. In the simulation, each amphiphilic lipid consists of a headgroup, which contains three connected hydrophilic beads, and two tails, which are connected to adjacent head beads with three hydrophobic beads per tail (see Figure 1a). The lipids are immersed in a hydrophilic solvent. Each Janus nanparticle is formed from 36 beads arranged on a FCC lattice; a cross section of the nanoparticle is shown in Figure 1b. The beads comprising a single nanoparticle are constrained to move as a rigid body. We verified that the solvent and lipid beads do not penetrate the interior of the nanoparticle. Specifically, we confirmed that such beads never enter or pass through the gaps between the beads forming the nanoparticles. The size of the nanoparticles is comparable to the thickness of the bilayer. In particular, the height of the nanoparticle (the distance between the tips of the vertical arrow) is 3 in DPD units. The ratio of hydrophobic to hydrophilic sites in the Janus nanoparticle is specified by the angle α.

Our three-dimensional simulation box is $40 \times 40 \times 20$ sites in size with periodic boundary conditions in all directions. At the beginning of our simulations, we distribute the lipids in two layers such that they form a stable, tensionless membrane, as shown in Figure 2a. When the Janus nanoparticles are introduced, they are initially located within the solvent. We stretch the membrane by changing the lateral dimensions of our simulation box and simultaneously modify the height of the box to keep the volume of the system constant. In particular, we start with a tensionless membrane where the area per lipid, A_0, is approximately $A_0 = 1.21$; we then increase the area of the box by 30% to create the pore. After a finite number of time steps, we reduce the box to its initial size. We then perform the second loading cycle, where the box area is increased by 15% relative to its initial size and again ultimately reduce the box size

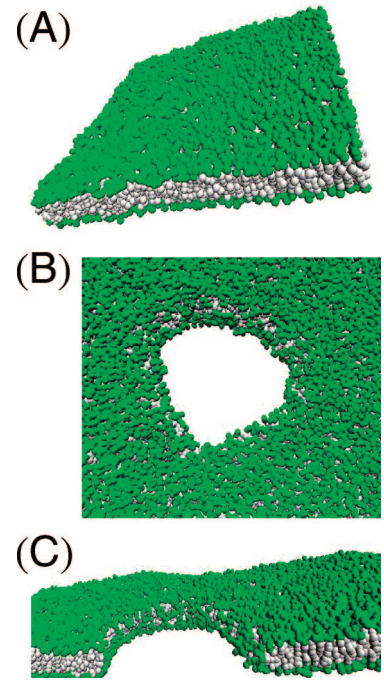

Figure 2. Snapshots of the pure lipid bilayer membrane (in the absence of the Janus nanoparticles). The green beads mark the hydrophilic head groups in the lipid, while the gray particles indicate the hydrophobic tails. The image in panel A shows a tensionless membrane. The images B and C show the hydrophilic pore that has formed in a stretched membrane from the top and in cross-section, respectively. Solvent is not shown.

to the initial parameters. The simulation is run for a sufficiently long time that there are no significant transient effects and the pore-containing membrane equilibrates into a stable structure.

RESULTS AND DISCUSSION

We first discuss the structural evolution of a membrane due to the imposed stretching in the absence the Janus particles and then describe the distinct differences in the behavior of the system due to the presence of the Janus nanoparticles. When a membrane is stretched, both the area per lipid and the membrane tension increase. The membrane tension increases nonlinearly for sufficiently large changes in the membrane area and results in membrane thinning. When the tension eventually exceeds a critical threshold, a small defect appears that perforates the membrane and causes it to be unstable, thus initiating the formation of a pore. Once the pore forms, the lipids rearrange to minimize the contact between the hydrophilic solvent and the lipids' hydrophobic tails. As can be seen in Figure 2b,c, the hydrophilic head groups point toward the solvent, forming a "hydrophilic" pore.

We characterize the pore formation in terms of the size of a pore opening, A_p, and the membrane tension, σ. Here, we plot A_p (in Figure 3) and σ (in Figure 4) as functions of the simulation time, together with a curve representing the changes in the dimensions of the

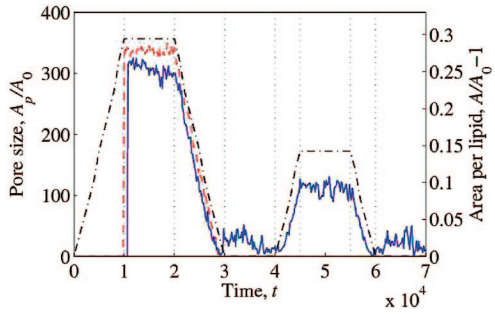

Figure 3. Size of a pore as a function of the simulation time. The red dashed line shows the pore size in a pure membrane; the blue solid line is for a membrane with 27 nanoparticles with $\alpha = 60°$. The dash−dotted line is for the normalized area per lipid and reflects the changes in the size of the simulation box. The vertical gray lines mark the times when the applied tension is altered.

simulation box. To estimate the pore opening A_p, we adopted the procedure proposed by Wang and Frenkel.[24]

As can be seen from Figures 3 and 4, the membrane ruptures and forms a pore when $\sigma \approx 5.3$ and the area per lipid is $A \approx 1.3A_0$. The size of the pore grows essentially instantaneously until it reaches its final size. (This rapid growth is driven by an imbalance in the forces at the edge of the pore; namely, until the system forms the structure in Figure 2b,c, the hydrophobic moieties are in contact with the hydrophilic solvent.) The stabilization of the pore is accompanied by a sharp decrease in membrane tension, as shown in Figure 4. In particular, the tension drops to approximately 0.5; the latter value is dictated by the line tension associated with the pore edge. The size of the open pore remains approximately equal to $335A_0$ while the simulation box is kept at the maximum extension.

When we reduce the size of the box, the pore shrinks at roughly the same rate as the box size is decreased. During this process, the membrane tension slightly increases and reaches a local maximum as the "hydrophilic pore" disappears. In particular, the lipids cannot readily reorganize to completely prevent contact between the solvent and the hydrophobic tails. This unfavorable contact increases the energy in the system and causes the increase in the membrane tension. The tension ultimately decreases as the pore completely closes and the external forcing is removed, and subsequently, σ fluctuates about zero, indicating that the restored membrane is unstressed.

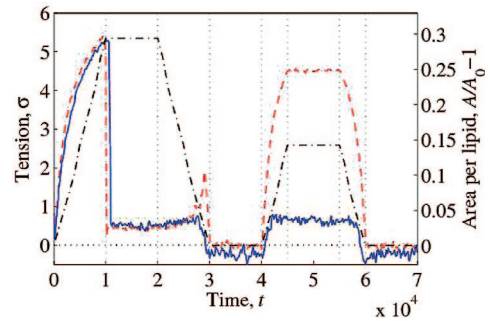

Figure 4. Dimensionless tension in the membrane as a function of the simulation time. The red dashed line shows the tension in a pure membrane; the blue solid line is for the tension in a membrane with 27 nanoparticles with $\alpha = 60°$. The dash−dotted line is for the normalized area per lipid and reflects the changes in the size of the simulation box. The vertical gray lines mark the times when the applied tension is altered.

In the second loading cycle, the maximum strain is set to a value that is below the threshold magnitude (*i.e.*, the value for rupturing the membrane). The membrane is stretched by about 15%, which induces a membrane tension of about 4.5. The membrane is able to withstand this tension (during the time scale of our simulations) without rupture and breakdown, *i.e.*, no pore appears in the membrane. When the stretching is removed, the shape of the membrane is restored to its preloading state. (We also note that there is no hysteresis between the loading and unloading cycles.)

Having considered the behavior of the isolated membrane, we are now in position to discuss the influence of Janus nanoparticles on the evolution of a stressed membrane. Into the surrounding solvent, we introduced 27 Janus nanoparticles that encompass a 60° hydrophobic part (*i.e.*, for each particle $\alpha = 60°$ in Figure 1b). This yields a concentration of roughly 1/100 nanoparticle per lipid. Since the concentration is relatively high, some nanoparticles aggregate within the solvent to form clusters of 4−6 particles, while some rapidly attach to the membrane. The latter nanoparticles diffuse in a random and independent fashion within the membrane, with their hydrophilic parts protruding into the solvent, and do not form any stable clusters or structures. We allow the nanoparticles to redistribute within the membrane and the bilayer to equilibrate before we apply the loading.

As can be seen in Figure 4, when the membrane is stretched in the beginning of the first loading cycle, the inclusion of the nanoparticles into the system essentially does not affect the evolution of the membrane tension. Moreover, the tension when the membrane bursts is almost identical in both the cases considered (with and without the particles). The size of the pore that is formed after the membrane bursts, however, is somewhat smaller for the membrane with the Janus nanoparticle. The smaller pore size is because the Janus nanoparticles diffuse and line the edge of the pore, with their hydrophilic portions extending into the solvent, as seen in Figure 5. The particles' hydrophobic moieties lie buried in the layer of tail groups. We find that the number of nanoparticles sitting at the edge of the pore increases with time.

The localization of Janus particles at the pore's edge lowers the free energy of the system and thus provides a driving force for the self-assembly of the particles in the pores. Indeed, when an opening forms, the lipids have to accommodate to the highly curved interface at the pore's edge, which has a curvature on the order of

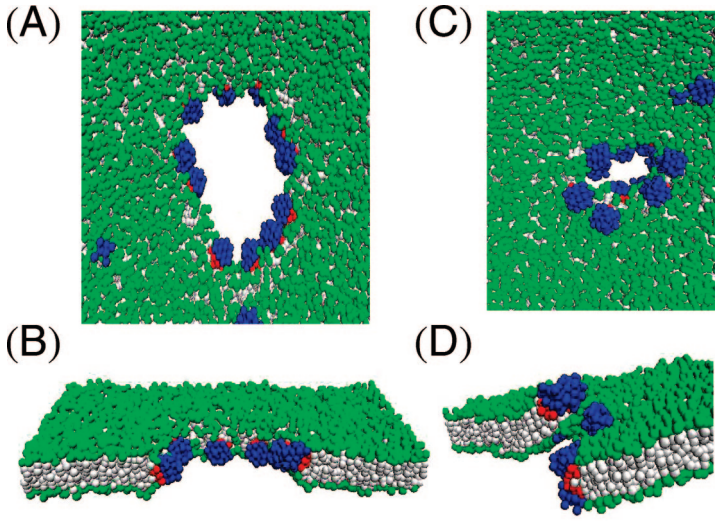

Figure 5. Snapshots of a lipid bilayer membrane in the presence of 27 nanoparticles with $\alpha = 60°$. The green beads mark the hydrophilic head groups in the lipid, while the gray particles indicate the hydrophobic tails. The blue beads mark the hydrophilic portion of the nanoparticles and the red beads indicate the hydrophobic portion. Snapshots A and B show a pore that was formed in a stretched membrane, where nanoparticles attach to the edge of the pore. Snapshots C and D show a nanoparticle-line pore formed when the membrane stretching is released. Solvent is not shown.

$(1/L_p)$, where L_p is the length of a lipid chain. On the other hand, when the Janus nanoparticles bind to the edge, the lipids can redistribute around the particles with a sufficiently lower curvature, and therefore, a lower energy. The nanoparticles could potentially completely cover the entire perimeter of a pore. This does not happen, however, due to thermal fluctuations. We did observe that about 10−12 nanoparticle attach simultaneously to an open pore and stably occupied more than a half of its perimeter (see Figure 5a).

When we reduce the membrane stretching, the size of the pore decreases and the nanoparticles approach each other quite closely, forming a ring at the pore edge. When the stretching is further reduced, some of the nanoparticles are pushed out of the ring and into the membrane. Eventually, when the box is restored to its initial size, about 6−8 nanoparticles form a cluster, which prevents the membrane from closing completely (see Figure 5c). Note that there is no increase in tension associated with the closing of a pore, as was observed in the pure membrane case (Figure 4). (The particles' hydrophilic portions remain localized in the hole, shielding the hydrophobic domain from the solvent.) Moreover, when the box assumes its initial size, there is a stable opening in the membrane due to the cluster of nanoparticles (Figure 5c,d) that have self-assembled at the interface.

We note also that tension in the membrane with the cluster of Janus beads is negative, indicating that the membrane is effectively compressed (Figure 4). Due to the compression, the membrane around the nanoparticle-decorated pore is deformed and takes on a three-dimensional shape, such that membrane sheets on the opposite sides of the cluster might overlap (see Figure 5d). In this case, no gap can be observed from the top view of the membrane, although there is still an opening that allows transport of the solvent through the membrane.

Another distinct feature due to the presence of the nanoparticle-lined pore is evident at the subsequent loading cycle. Even when the stretching is not sufficient to cause a rupture of a pure membrane, the membrane with an attached cluster of nanoparticles readily forms a wide opening when the membrane is stretched. Moreover, the size of the pore is directly proportional to the magnitude of the stretching, and thus, can be readily regulated. Similar to the events in the first loading cycle, additional particles diffusing in the membrane attach to the edge of a wide, open pore. When the box size is restored, the Janus species again form a cluster of attached particles that prevent the full closure of the opening. This behavior indicates that the particle-decorated pore can undergo multiple opening and closing cycles, as was indeed observed in the simulations.

We note that in our simulations, the nanoparticles were not able to nucleate pores within the bilayer; the stretching of the membrane to create an initial opening was necessary for forming the particle-decorated holes. This indicates that there is an energy barrier, which prevents the spontaneous formation of the particle-decorated pores, and the initial stretching and bursting of the lipid membrane are essential steps in the process.

To probe the effect of the particle concentration on the assembly of the species in the pore, we varied the volume fraction of Janus particles in our simulation. We found that as few as four nanoparticles is sufficient to form a particle-lined pore. These nanoparticles organize in two closely located pairs, in which the hydrophilic parts of the particles point to the opposite sides of the membrane, as shown in Figure 6a. In this scenario, no opening prevails in the compressed membrane (Figure 6b). Minor stretching, however, is able to create an open pore (Figure 6c), similar to that observed for larger concentrations of nanoparticles.

We also studied the effect of the nanoparticle's composition on the process of pore formation. Specifically, we changed the relative distribution of hydrophilic and hydrophobic moieties on the surface of the particle. Our simulations with 27 Janus particles revealed that stable pores appear with nanoparticles having a 30° hydrophobic portion (*i.e.*, $\alpha = 30°$). In this case, however, the nanoparticles do not prevent the complete closing of the pore; rather, the particles form a cluster that serves as a nucleation defect in the membrane and, thus, allows pore opening for lower magnitudes of stretching.

Nanoparticles with a 90° hydrophobic part also diffuse to the edge of an open pore and form clusters

when the stretching is released. These clusters, however, are unstable and disassemble after a relatively short period of time. Thus, a membrane with $\alpha = 90°$ nanoparticles can be readily reopened only a short time after the tension is removed. Moreover, we did not observe particle attachment to the edge of an open pore for Janus particles with either a 120° or 150° hydrophobic cap. Although such nanoparticles easily bind to the membrane, they cannot form a cluster and only slightly affect the entire evolution of the membrane by decreasing its area per lipid.

The above findings indicate that Janus nanoparticles with a 60° hydrophobic portion are close to the optimal composition (for a given particle size) for forming stable pores in amphiphilic membranes. This distribution between the hydrophilic and hydrophobic moieties allows the amphiphilies to accommodate the nanoparticles at a pore edge with the minimum energy as compared to other particle compositions, thus creating an energy barrier sufficient to prevent membrane closure due to thermal fluctuation and even compression by an external forcing.

In summary, using computational modeling, we have shown that Janus particles in solution will localize to the edges of a pore in a lipid bilayer membrane. The Janus nanoparticles stabilize the pore location and size so that material can perform in a reliable, repeatable manner; it is this critical feature that the Janus particles contribute to the system. The amphiphilic nature of the Janus particles is crucial for this behavior since portions of the particles must interface with the hydrophobic regions and certain regions must interface with the aqueous solution in the hole.

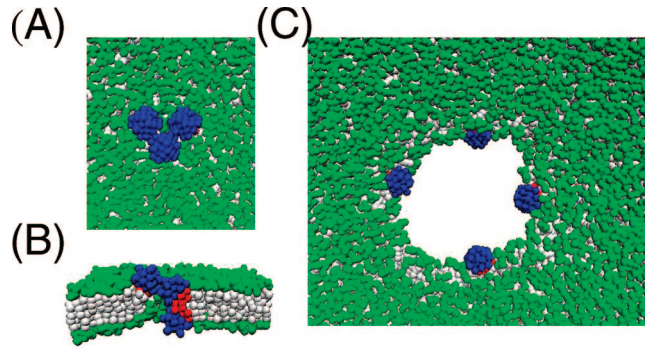

Figure 6. Snapshots of a lipid bilayer membrane with four nanoparticles with $\alpha = 60°$. The particles are as in Figure 5. Snapshots A and B show the nanoparticles assembled in a cluster that perforates the unstretched membrane and serves as a nucleation site for pore opening. Snapshot C shows a pore in a stretched membrane. Solvent is not shown.

In essence, the Janus particles introduce a controllably "re-sealable" pore in the membrane. It is this attribute that makes the assembly a viable component in self-regulating materials, where the pores would remain open under one set of conditions, but close with a change in the surroundings. For example, a change in temperature,[25] pH[26] or salt concentration (or osmotic pressure)[27] could be harnessed to increase the area per chain. The latter increase would in term increase the membrane tension, driving the particle-lined pores to open. As these variations in the solution dissipate, the area per chain (membrane tension) is restored and the particle-lined pore would close. It is in this manner that variations in the external conditions could be harnessed to drive the opening or closing of the Janus particle-decorated pore.

METHODS

To model the interactions among the lipid bilayer, nanoscopic particles, and solvent, we apply the dissipative particles dynamics (DPD) technique. DPD is a coarse-grained molecular dynamics (MD) approach that can capture effectively the hydrodynamics of complex fluids while retaining essential information about the structural properties of system's component. DPD was first introduced by Hoogerbrugge and Koelman[28] and then shown to be a useful tool for simulating a host of multicomponent systems, including the evolution of various lipid membranes.[14–22] An advantageous feature of DPD is that it utilizes soft repulsive interactions between the beads, which represent clusters of molecules. Consequently, one can use a significantly larger time step Δt between successive iterations than those required by MD simulations. This, in turn, allows this approach to be used for modeling physical phenomena occurring at time and spatial scales many orders of magnitude greater than that captured by MD.

Similar to MD simulations, DPD captures the time evolution of a many-body system through the numerical integration of Newton's equation of motion, $m\, d\mathbf{v}_i/dt = \mathbf{f}_i$, where the mass m of a bead of any species is set to one. (We use the term "bead" to refer to a single point particle in the numerical simulation and the term "particle" to refer to a nanoparticle.) Unlike MD simulations, DPD involves the use of soft, repulsive interactions (as noted above) and a momentum-conserving thermostat. The force acting on a bead contains three parts, each of which is pairwise additive: $\mathbf{f}_i(t) = \sum(\mathbf{F}_{ij}^{C} + \mathbf{F}_{ij}^{D} + \mathbf{F}_{ij}^{R})$, where the sum runs over all beads j within a certain cutoff radius r_c. The conservative force is a soft, repulsive force given by $\mathbf{F}_{ij}^{C} = a_{ij}(1 - r_{ij})\hat{\mathbf{r}}_{ij}$, where a_{ij} is the maximum repulsion between beads i and j, $r_{ij} = |\mathbf{r}_i - \mathbf{r}_j|/r_c$, and $\hat{\mathbf{r}}_{ij} = \mathbf{r}_{ij}/|\mathbf{r}_{ij}|$. The drag force is $\mathbf{F}_{ij}^{D} = -\gamma\omega_D(r_{ij})(\hat{\mathbf{r}}_{ij} \cdot \mathbf{v}_{ij})\hat{\mathbf{r}}_{ij}$, where γ is a simulation parameter related to viscosity, ω_D is a weight function that goes to zero at r_c, and $\mathbf{v}_{ij} = \mathbf{v}_i - \mathbf{v}_j$. The random force is $\mathbf{F}_{ij}^{R} = \phi\, \omega_R(r_{ij})\xi_{ij}\hat{\mathbf{r}}_{ij}$, where ξ_{ij} is a zero-mean Gaussian random variable of unit variance and $\phi^2 = 2k_BT\gamma$. Finally, we use $\omega_D(r_{ij}) = \omega_R(r_{ij})^2 = (1 - r_{ij})^2$ for $r_{ij} < r_c$. Because all three of these forces conserve momentum locally, hydrodynamic behavior emerges even in systems containing only a few hundred particles.[14] The equations of motion are integrated in time with a modified velocity−Verlet algorithm.[11]

We take r_c as the characteristic length scale and k_BT as the characteristic energy scale in our simulations. A characteristic time scale is then defined as $\tau = \sqrt{mr_c^2/k_BT}$. The remaining simulation parameters are $\phi = 3$ and $\Delta t = 0.02\tau$ with a total bead number density of $\rho = 3/r_c^3$.

As shown in Figure 1A, our system contains short-chain lipids. The bonds between beads in the chain are represented by the harmonic spring potential $E_{bond} = K_{bond}((r - b)/r_c)^2$, where K_{bond} is the bond constant and b is the equilibrium bond length. We use $K_{bond} = 64$ and $b = 0.5$. We also insert a weaker bond ($K'_{bond} = 16$) between the first beads on the two tails to keep the tails oriented in the same direction. Additionally, we include a three-body stiffness potential along the tails of the form $E_{angle} = K_{angle}(1 + \cos\ \theta)$ where θ is the angle formed by three adjacent beads and we set the coefficient to $K_{angle} = 20$. This stiff-

ness term increases the stability and bending rigidity of the bilayers.

The amphiphilic nature of the lipids is captured by specifying the repulsive interactions between the components. For any two beads of the same type, we take the repulsion parameter to be $a_{ii} = 25$. Given that S stands for solvent, H stands for head and T stands for tail, we set the remaining interactions to the following: $a_{HS} = 25$, $a_{HT} = 100$, and $a_{ST} = 100$. At these values, we find that lipids spontaneously self-assemble into bilayers, as has previously been observed for similar values.[11,14]

Each Janus particle is a nearly spherical solid, which is formed from 36 particle beads arranged on a FCC lattice with a number density of $\rho = 3/r_c^3$. The Janus nanoparticle is also composed of hydrophobic and hydrophilic regions. We set the repulsive interaction of the particle's hydrophobic surface region with the aqueous solution and with the lipid head groups to 100. The interaction between the particle's hydrophobic domain and the lipid tails is 25. With respect to the hydrophilic portion of the particle, we use 100 to model its interaction with the hydrophobic lipid tails, whereas all other interactions are set to 25. As noted above, the corresponding values were used to induce the spontaneous self-assembly of the lipid bilayers and thus, they serve to capture the inherent incompatibility between the hydrophobic and hydrophilic components.[11,14]

The simulation results can be related to physical length and time scales by examining the properties of a tensionless membrane.[11] Typical experimental measurements of dipalmitoylphosphatidylcholine (DPPC) membranes[29] in a tensionless state yield an equilibrium area per lipid of approximately 0.6 nm^2. We used this value to establish a length scale in our previous DPD simulations,[11] and thereby set $r_c = 0.67$ nm. We estimated the DPD time scale τ from the in-plane diffusion constant of lipids, which, for a flat DPPC membrane, has been measured[29] as $D = 5\ \mu m^2/s$. Matching this to the diffusion constant in a simulation yielded $\tau = 7.2$ ns and, for a single time step, $\Delta t = 0.02\tau = 0.14$ ns.

Acknowledgment. The authors gratefully acknowledge funding from ARO (to A.A.) and NSF (to W.U.) and thank Drs. Kurt Smith and Victor Yashin for helpful conversations.

REFERENCES AND NOTES

1. For a recent review see: Chan, D. I.; Prenner, E. J.; Vogel, H. J. Tryptophan- and Arginine-rich Antimicrobial Peptides: Structures and Mechanisms of Action. *Biochim. Biophys. Acta* **2006**, *1758*, 1184–1202.
2. Livadaru, L.; Kovalenko, A. Fundamental Mechanism of Translocation Across Liquidlike Membranes: Toward Control Over Nanoparticle Behavior. *Nano Lett.* **2006**, *6*, 78–83.
3. Herant, M.; Heinrich, V.; Dembo, M. Mechanics of Neutrophil Phagocytosis: Experiments and Quantitative Models. *J. Cell Sci.* **2006**, *119*, 1903–1913.
4. Deserno, M. Elastic Deformation of a Fluid Membrane Upon Colloid Binding. *Phys. Rev. E* **2004**, *69*, 031903.
5. Deserno, M.; Bickel, T. Wrapping of a Spherical Colloid by a Fluid Membrane. *Europhys. Lett.* **2003**, *62*, 767–773.
6. Deserno, M.; Gelbart, W. M. Adhesion and Wrapping in Colloid-Vesicle Complexes. *J. Phys. Chem. B* **2002**, *106*, 5543–5552.
7. Fleck, C. C.; Netz, R. R. Electrostatic Colloid-Membrane Binding. *Europhys. Lett.* **2004**, *67*, 314–320.
8. Harden, J. L.; MacKintosh, F. C.; Olmsted, P. D. Budding and Domain Shape Transformations in Mixed Lipid Films and Bilayer Membranes. *Phys. Rev. E* **2005**, *72*, 011903.
9. Bozic, B.; Kralj-Iglic, V.; Svetina, S. Coupling Between Vesicle Shape and Lateral Distribution of Mobile Membrane Inclusions. *Phys. Rev. E* **2006**, *73*, 041915.
10. Lipowsky, R.; Dobereiner, H. G. Vesicles in Contact with Nanoparticles and Colloids. *Europhys. Lett.* **1998**, *43*, 219–225.
11. Smith, K. A.; Jasnow, D.; Balazs, A. C. Designing Synthetic Vesicles That Engulf Nanoscopic Particles. *J. Chem. Phys.* **2007**, *127*, 084703.
12. Noguchi, H.; Takasu, M. Adhesion of Nanoparticles to Vesicles: A Brownian Dynamics Simulation. *Biophys. J.* **2002**, *83*, 299–308.
13. Ginzburg, V. V.; Balijepalli, S. Modeling the Thermodynamics of the Interaction of Nanoparticles with Cell Membranes. *Nano Lett.* **2007**, *7*, 3716–3722.
14. Illya, G.; Lipowsky, R.; Shillcock, J. C. Effect of Chain Length and Asymmetry on Material Properties of Bilayer Membranes. *J. Chem. Phys.* **2005**, *122*, 244901.
15. Groot, R. D.; Rabone, K. L. Mesoscopic Simulation of Cell Membrane Damage, Morphology Change and Rupture by Nonionic Surfactants. *Biophys. J.* **2001**, *81*, 725–736.
16. Venturoli, M.; Smit, B.; Sperotto, M. M. Simulation Studies of Protein-Induced Bilayer Deformations, and Lipid-Induced Protein Tilting, on a Mesoscopic Model for Lipid Bilayers with Embedded Proteins. *Biophys. J.* **2005**, *88*, 1778–1798.
17. Yamamoto, S.; Hyodo, S. Budding and Fission Dynamics of Two-Component Vesicles. *J. Chem. Phys.* **2003**, *118*, 7937–7943.
18. Yamamoto, S.; Maruyama, Y.; Hyodo, S. Dissipative Particle Dynamics Study of Spontaneous Vesicle Formation of Amphiphilic Molecules. *J. Chem. Phys.* **2002**, *116*, 5842–5849.
19. Laradji, M.; Sunil Kumar, P. B. Dynamics of Domain Growth in Self-Assembled Fluid Vesicles. *Phys. Rev. Lett.* **2004**, *93*, 198105.
20. Shillcock, J. C.; Lipowsky, R. Equilibrium Structure and Lateral Stress Distribution of Amphiphilic Bilayers From Dissipative Particle Dynamics Simulations. *J. Chem. Phys.* **2002**, *117*, 5048–5061.
21. Kranenburg, M.; Venturoli, M.; Smit, B. Molecular Simulations of Mesoscopic Bilayer Phases. *Phys. Rev. E* **2003**, *67*, 060901.
22. Rekvig, L.; Kranenburg, M.; Vreede, J.; Hafskjold, B.; Smitt, B. Investigation of Surfactant Efficiency Using Dissipative Particle Dynamics. *Langmuir* **2003**, *19*, 8195–8205.
23. Groot, R. D.; Warren, P. B. Dissipative Particle Dynamics: Bridging the Gap Between Atomistic and Mesoscopic Simulation. *J. Chem. Phys.* **1997**, *107*, 4423–4435.
24. Wang, Z. J.; Frenkel, D. Pore Nucleation in Mechanically Stretched Bilayer Membranes. *J. Chem. Phys.* **2005**, *123*, 154701.
25. Jain, M.; Wagner, R. C. *Introduction to Biological Membranes*; John Wiley & Sons, Inc.: New York, 1980.
26. Petelska, A. D.; Figaszewski, Z. A. Effect of pH on the Interfacial Tension of Lipid Bilayer Membrane. *Biophys. J.* **2000**, *78*, 812–817.
27. See for example: Idiart, M. A.; Levin, Y. Rupture of a Liposomal Vesicle. *Phys. Rev. E* **2004**, *69*, 061922.
28. Hoogerbrugge, P. J.; Koelman, J. Simulating Microscopic Hydrodynamic Phenomena with Dissipative Particle Dynamics. *Europhys. Lett.* **1992**, *19*, 155–160.
29. Shillcock, J. C.; Lipowsky, R. Tension-Induced Fusion of Bilayer Membranes and Vesicles. *Nat. Mater.* **2005**, *4*, 225–228.